

# Manipulation of Individual Carbon Nanotubes and Their Interaction with Surfaces

Tobias Hertel, Richard Martel, and Phaedon Avouris\*

IBM Research Division, T. J. Watson Research Center, Yorktown Heights, New York 10598

Received: October 28, 1997; In Final Form: December 16, 1997

We demonstrate that the tip of an atomic force microscope (AFM) can be used to control the shape and position of individual multiwalled carbon nanotubes dispersed on a surface. Specifically we can bend, straighten, translate, rotate, and—under certain conditions—cut nanotubes. Such manipulations are feasible due to the interaction between nanotubes and the substrate, which can stabilize highly strained nanotube configurations. Direct evidence for this interaction is provided by the study of elastic distortions of tubes interacting with other tubes and the substrate. From the observed deformations of nanotubes with 100 Å diameter, for example, we obtain a binding energy of  $0.8 \pm 0.3$  eV/Å. This interaction forces nanotubes to conform to the structure of the substrate, and the resulting distortions should induce corresponding changes in their electronic structure and electrical transport properties.

## I. Introduction

Carbon nanotubes with their unique mechanical<sup>1–5</sup> and electrical<sup>6–13</sup> properties are promising candidates for novel nanoelectronic devices. Because of their electric transport characteristics, which, depending on their structure, range from metallic to semiconducting, these materials can be used, for example, as nanowires<sup>6–10</sup> or as metal/semiconductor heterojunctions.<sup>11,12</sup> Carbon nanotubes were, however, found to exhibit large variations in their resistivity, a fact which can be attributed to structural defects or, as we discuss here, elastic deformations.<sup>6,8,13</sup>

Progress toward structurally well-defined nanotube samples recently has been achieved by the synthesis of single-walled nanotubes, a high content of these having identical molecular structure.<sup>14</sup> However, presently there is little control over the alignment and shape of absorbed nanotubes. Electric transport through nanotubes<sup>7–10</sup> was studied after their random deposition on a substrate bearing electrical contacts and thus relied on chance that a nanotube with the proper alignment would be found. Such studies will greatly benefit from schemes that allow the control of the position and shape of the nanotubes. This is of course also essential if the nanotubes are to be used in any future device technology.

In this study we demonstrate that the tip of an AFM can be used to manipulate multiwalled carbon nanotubes on a passivated silicon surface. The interaction between nanotubes and the surface is crucial for such manipulations. We show how the strength of the nanotube–surface interaction can be determined from the observed elastic deformations of tubes on the surface.

## II. Results and Discussion

The multiwalled nanotubes used for this study were dissolved in methylene chloride using an ultrasonic bath. The solution was dispersed on a H-passivated Si(100) surface. Imaging and manipulation was performed in air using an atomic force microscope.

Most discussions of the structure and associated properties of nanotubes refer to isolated (unsupported) nanotubes. Supported nanotubes, however, should interact strongly with the substrate, and as a result a number of deformations may arise. The AFM images of nanotubes shown in Figure 1 illustrate different types of elastic deformations observed on the freshly covered surface and after manipulation with the AFM tip. Figure 1a shows how nanotubes crossing one another are deformed elastically due to their interaction with the surface—despite their exceptionally large Young's modulus of about 1.5 TPa.<sup>1,4</sup> The attractive interaction with the substrate forces the upper nanotube along profile 2 in Figure 1a to maximize its area of contact with the surface at the expense of strain energy building up when it flexes around a lower nanotube. Profile 1 illustrates how a nanotube can also be compressed elastically under the load of another nanotube lying on top of it. The strength of the attractive forces between nanotubes and the surface can be estimated using a quasi one-dimensional model where the profile  $d(x)$  along the tube principal axis is determined by the balance of strain and adhesion energies  $E_\epsilon + E_{ad}$ . We calculate the profile  $d(x)$  by minimizing the total energy of a one-dimensional tube that is crossing a pointlike obstacle of given height. We obtain the strain energy  $E_\epsilon$  by integration of  $E\pi(a^4 - b^4)/8\int r(x)^{-2} dx$  over the length of the tube where  $E$  is Young's modulus,  $a$  and  $b$  give the outer and inner nanotube radii, respectively and  $r(x)$  is the local radius of curvature along the principal axis ( $b^4$  is assumed to be significantly smaller than  $a^4$  and thus can be neglected).<sup>15</sup> The outer tube radius  $a$  was determined from the apparent height of nanotubes in our AFM images.<sup>16</sup> In principle, the binding energy can be determined by short-ranged chemical and long-ranged van der Waals interactions, and the corresponding forces may be modeled using appropriate potentials. The simulations revealed, however, that the profile  $d(x)$  depends only on the depth of the potential minimum and is independent of the particular potential shape. An investigation of tube profiles such as the one shown in Figure 1a, therefore, provides a unique way to determine the substrate–nanotube binding energy. The profile  $d(x)$  has been determined experimentally for various tube diameters and obstacle heights to be compared to a number of

\* To whom correspondence should be addressed.

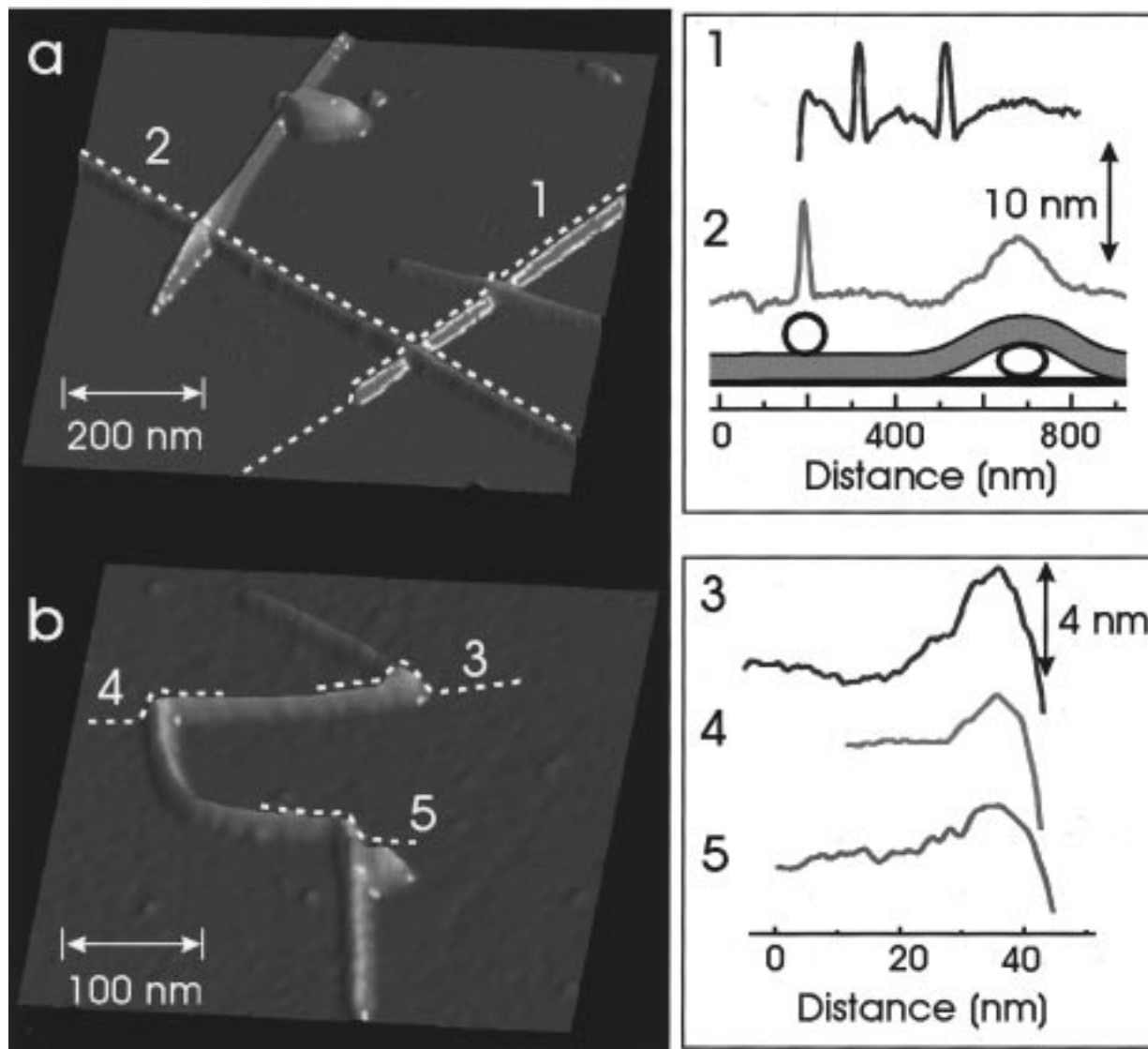


**Figure 1.** Noncontact AFM images of elastically deformed nanotubes on a hydrogenated Si(100) surface. For imaging in the noncontact mode the tip is scanned across the sample at a distance of about 30 Å so that vertical forces between tip and surface are extremely small (typically about 5 pN). (a) The height of the nanotube along profile 1 is reduced by at least 30 Å in the vicinity of the contact with another nanotube crossing on top. The height at the crossing point is also found to be reduced by almost 60 Å with respect to the sum of the individual nanotube diameters. (b) Strongly bent nanotube with buckling of 15 Å up to 35 Å in heavily strained regions. The amount of buckling correlates with the bending angle (profiles 3–5).

different configurations such as the one shown in Figure 1a. For nanotubes with a diameter of about 100 Å, we obtain a binding energy of  $0.8 \pm 0.3$  eV/Å. These results are confirmed by molecular mechanics simulations of single and multiwalled carbon nanotubes bonded by van der Waals forces to a graphite surface.<sup>17</sup> An important consequence of this large binding energy is that nanotubes will tend to distort and conform to the substrate topography.

The experimentally obtained binding energy of 0.8 eV/Å also allows us to estimate the forces at nanotube/nanotube/substrate contacts like the ones in Figure 1a by using the calculated change of the total energy when the height of the lower tube is reduced. The resulting force acting at the point of contact in Figure 1a is about 35 nN. Such strong forces are due to a substantial increase of the contact area of the upper tube with the substrate, and thus a gain in binding energy, when the obstacle height is reduced. This implies that the pressure between nanotubes at these contacts can reach about 10 GPa, which is evident from the strong compression of the lower nanotube seen in profile 1 of Figure 1a. Such enormous

pressures are known to lead to drastic modifications of the bonding and electrical properties of carbon compounds.<sup>18,19</sup> For single-walled nanotubes with a diameter of 13 Å (e.g. a (10,-10) nanotube), the force to compress them by 30% should be of the order of 10 nN so that the tip of an AFM may well be used to locally perturb their geometric and electronic structure (this is estimated using the curvature modulus of 1.4 eV<sup>20</sup>). The interaction of nanotubes with the surface should also have consequences for the electrical transport through overlapping nanotube segments if connections of this kind are established between different nanotubes on a surface.

The observed strong interaction of nanotubes with the surface determines both the normal force that binds them to the substrate and the pinning forces that are responsible for frictional properties when nanotubes are moved laterally across the surface. This interaction is, therefore, also crucial for any attempt to manipulate nanotubes with the AFM tip and for stabilization of nanotubes in strained configurations. Evidence for the strength of the frictional forces can be obtained from images of nanotubes after they have been perturbed by scanning

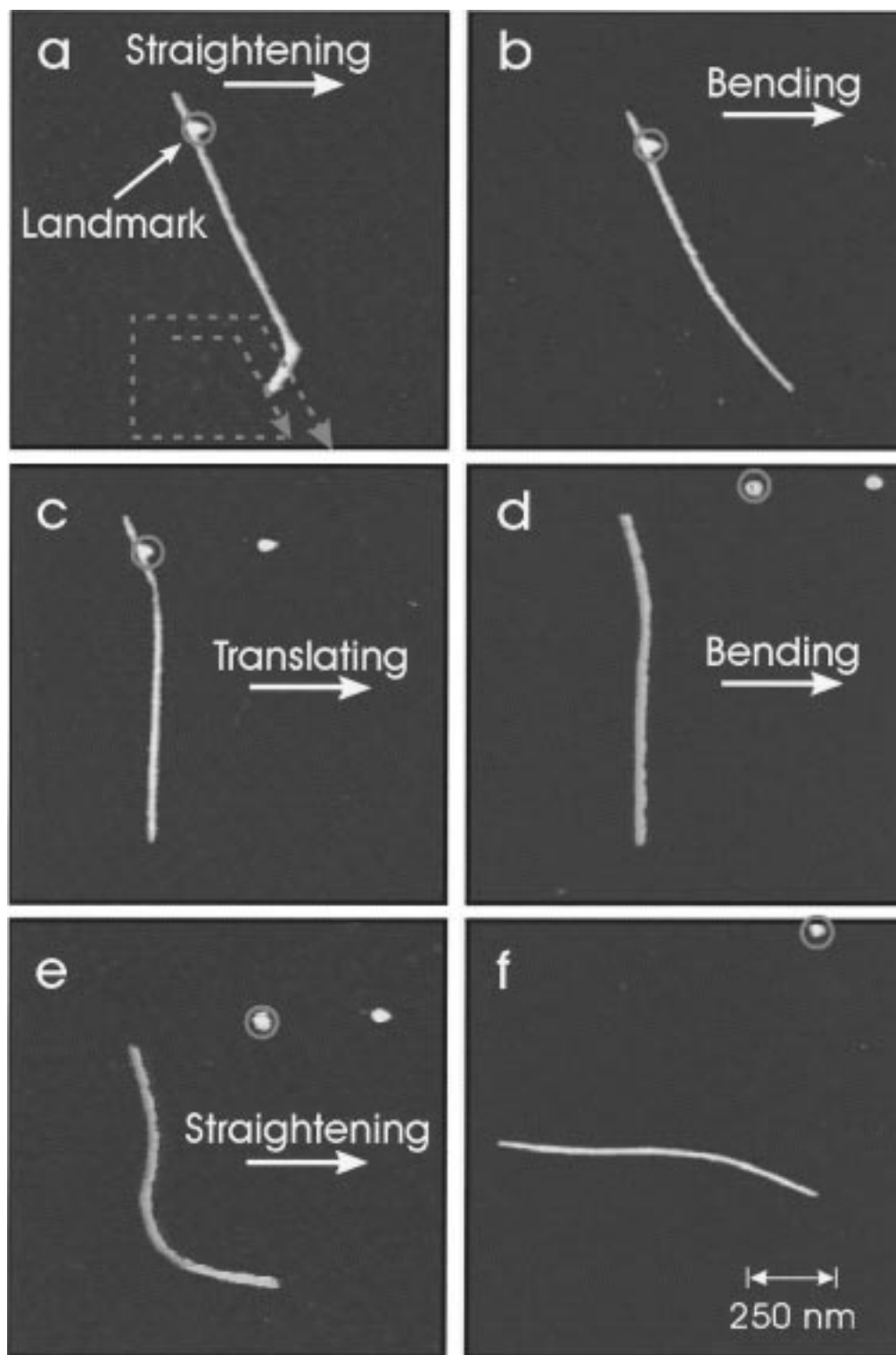


**Figure 2.** Manipulation of a  $0.9 \mu\text{m}$  long and  $80 \text{ \AA}$  high nanotube at a vertical load of 20 nN. (a,b) A strongly bent nanotube segment can be straightened by repeated movement of the tip parallel to the nanotube axis (dashed line). Every move brings the nanotube successively closer to the desired geometry. (c–f) The nanotube can also be realigned vertically, translated, bent and rotated around the surface normal.

the surface with the AFM tip in contact. In this mode, the loading force between tip and surface of 20 nN provides lateral forces strong enough to cause bending and displacement of nanotubes. Figure 1b reproduces one of many examples where a nanotube has been bent so strongly that curved segments start to buckle and form kinks in a manner similar to that reported recently.<sup>5</sup> The observed correlation between bending angle and buckling height in Figure 1b suggests a successive vertical compression of the nanotube in the kinked region. Our studies

show that such kinked nanotubes can be straightened by controlled manipulation without structural damage visible at the resolution provided by the AFM. High-resolution transmission electron micrographs, however, indicate that some of the strain in strongly bent nanotube segments may also be relieved by stress fracture in addition to elastic deformations.<sup>21</sup> Given the dependence of chemical reactivity on bond strain, one could perhaps exploit the ability to produce locally strained nanotube configurations with the AFM tip to induce local chemistry.

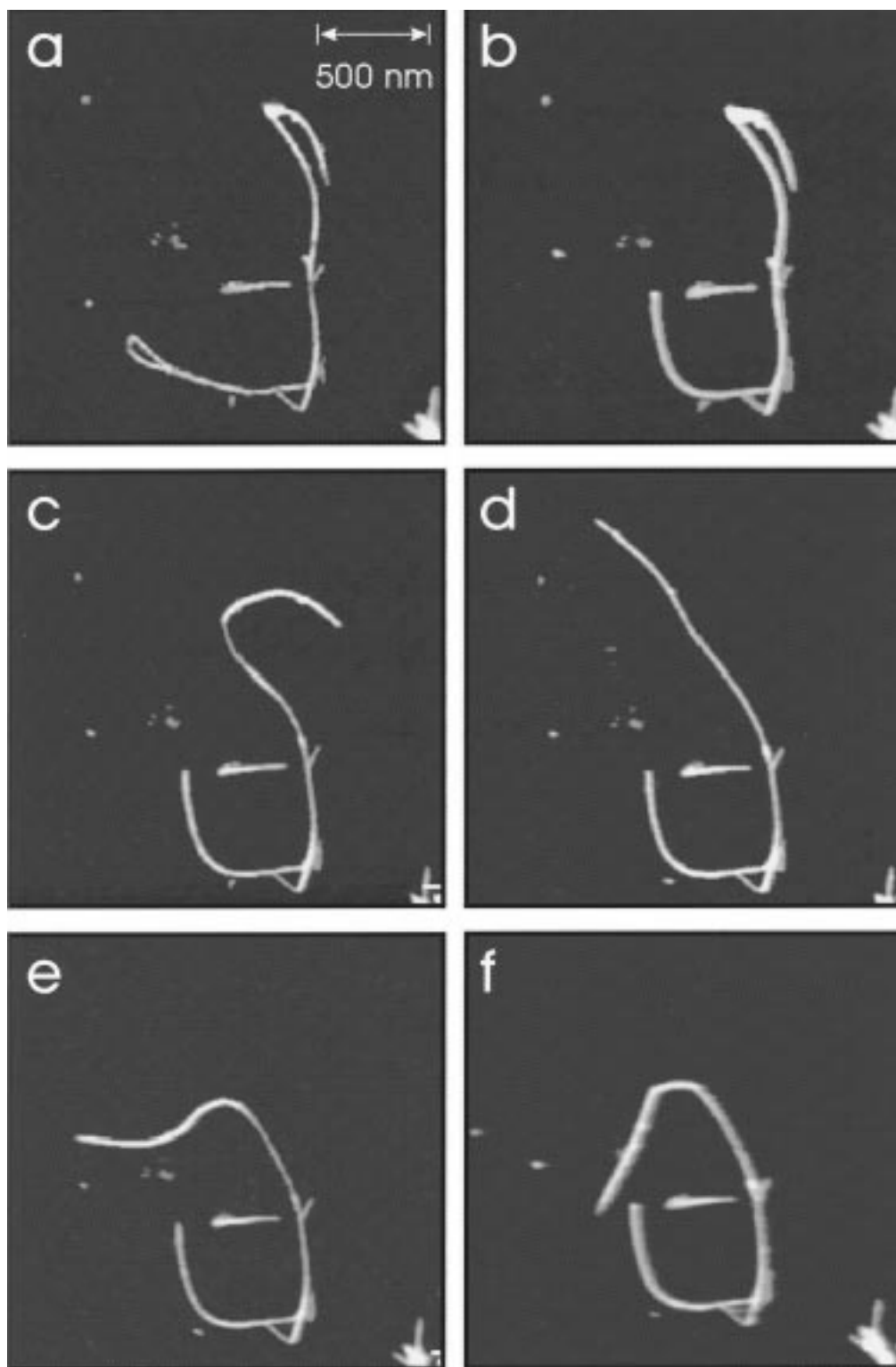


**Figure 3.** Fabrication of a more complex pattern (the Greek letter  $\Theta$ ) from a nanotube structure with a total length of about  $2.5 \mu\text{m}$ , possibly consisting of more than one individual nanotube (not all steps are shown).

When scanning the surface in the contact AFM mode, we found that nanotubes can be displaced on the surface in a controlled manner similar to recent manipulations of molecules with an STM.<sup>22</sup> In addition to the rigid displacement of molecules, the nanotubes could be bent and realigned. This encouraged us to attempt controlled manipulation of the shape, position, and alignment of nanotubes by pushing nanotube segments in a predefined way. First, the area of interest is imaged in the noncontact mode and then the contact mode, was employed in order to apply higher vertical and lateral forces.

The images in Figure 2 demonstrate how the nanotube can be realigned vertically, translated, bent, and then rotated (around the surface normal). These results prompted us to further test the performance of the manipulation technique by fabricating a more complex pattern. Figure 3a–f shows how we realigned a nanotube bundle in several steps to form the Greek letter  $\Theta$ . These results confirm the ability of the AFM tip as a tool to manipulate individual nanotubes or bundles in a controlled way.

Quantitative information on lateral (frictional) forces is obtained from images of bent nanotubes such as the one shown

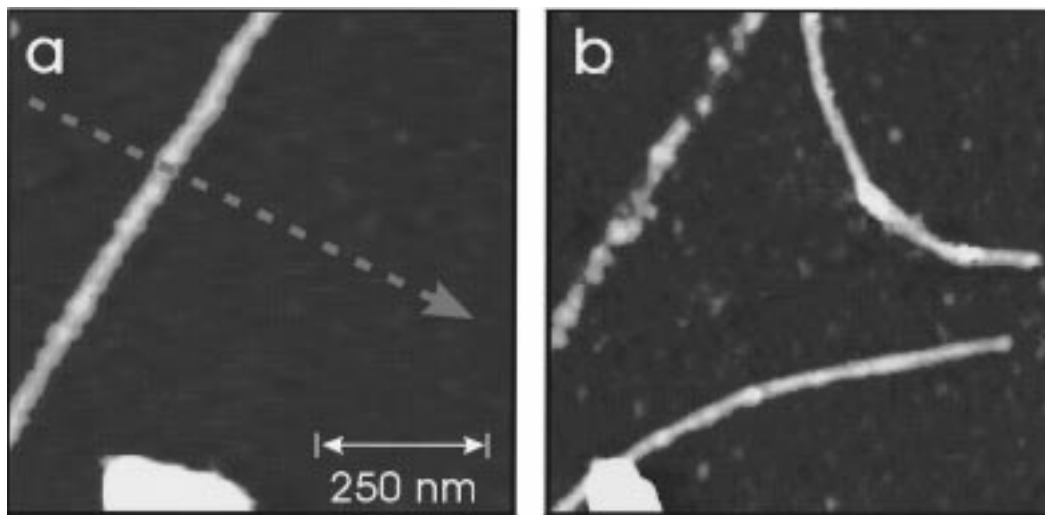


**Figure 4.** Nanotube dissection. If a nanotube is pinned strong enough to the surface it can occasionally also be cut by crossing the tube with the tip in contact as indicated by the red arrow.

in Figure 2e. These configurations can possess strain energies of several hundred electronvolts and have to be pinned in this shape either by the corrugation of the surface potential or by interaction with defects. The force  $F$  required to keep the nanotube of Figure 2e in place has to be about 5 nN if it is evenly distributed along the whole length of the lower bent segment. As a result of the strong nanotube–surface interaction, the nanotube should be flattened on the surface side so as to increase the effective area of contact. Molecular mechanics calculations indicate that the width of the contact region can lie between 5% and 50% of the nanotube diameter, depending on the tube radius and number of shells.<sup>17</sup> Thus, using the estimated contact area  $A$  of  $5 \times 10^{-16} \text{ m}^2$  for the lower tube segment in Figure 2e we obtain a shear stress  $\sigma = F/A$  of  $10^7 \text{ N/m}^2$ . This compares well, for example, with the shear strength of graphite of  $1.03 \times 10^7 \text{ N/m}^2$ .<sup>23</sup>

To obtain control over the length of nanotubes, we made an effort to dissect long nanotubes with comparatively small diameter ( $\sim 40 \text{ \AA}$ ) by pulling the tip in contact across the nanotube on the surface. In most attempts the nanotube could not be cut but instead was dragged across the surface. Images taken during a successful cutting experiment (Figure 4) show that the nanotube was significantly stretched before it eventually broke. In this particular case, however, the nanotube was contaminated with amorphous carbon, as seen from the spotty line left behind at its original position. This contamination may have increased its adhesion to the substrate. We note that this type of contamination was not found in other experiments presented here as can be seen from the absence of such spotty lines in Figures 2 and 3.

### III. Conclusions

We showed that the interaction of nanoscaled objects such as nanotubes with a surface can lead to substantial binding energies of  $0.8 \pm 0.3 \text{ eV/\AA}$  for nanotubes with  $100 \text{ \AA}$  apparent diameter, for example. As a consequence nanotubes tend to distort so as to conform to the topography of the substrate. Such distortions can have implications for the electrical properties of nanotubes. Studies on electrical transport through supported carbon nanotubes such as the ones described in refs 6–10 are usually performed on lithographically patterned insulator surfaces. The flexing of a nanotube over sharp features such as electrical leads produces regions of increased curvature and, therefore, stronger  $\pi$ – $\sigma$  interactions and  $sp^2$  to  $sp^3$  rehybrid-

ization. Such interactions lead to a variation of the local density of states along the tube, and the formation of interface dipoles between bent and straight nanotube sections, effects that should modify electrical transport properties.<sup>24</sup>

We found that we can manipulate and elastically deform nanotubes not only on hydrogenated silicon but also on  $\text{SiO}_2$  surfaces, indicating that the corresponding frictional forces (intrinsic or defect induced) are likewise strong enough to pin nanotubes in strained configurations. Future investigations can, therefore, benefit from the presented manipulation schemes, which may allow the study of electrical properties of nanotubes as a function of their shape and alignment.

**Acknowledgment.** We thank R. Smalley for stimulating our interest in carbon nanotubes, B. Persson for helpful discussion and critical comments, and H. Dai for providing us with a sample of multiwalled carbon nanotubes. Helpful discussions with T. Schmidt are also acknowledged. T.H. acknowledges financial support by the Alexander von Humboldt foundation and the Max-Planck-Society.

### References and Notes

- (1) Treacy, M. M. J.; Ebbesen, T. W.; Gibson, J. M. *Nature* **1996**, *381*, 678–680.
- (2) Iijima, S.; Brabec, C.; Maiti, A.; Bernholc, J. *J. Chem. Phys.* **1996**, *104*, 2089–2092.
- (3) Yakobson, B. I.; Brabec, C. J.; Bernholc, J. *Phys. Rev. Lett.* **1996**, *76*, 2511–2514.
- (4) Wong, E. W.; Sheehan, P. E.; Lieber, C. M. *Science* **1997**, *277*, 1971–1975.
- (5) Falvo, M. R.; Clary, G. J.; II, R. M. T.; Chi, V.; Brooks, F. P., Jr.; Washburn, S.; Superfine, R. *Nature* **1997**, *389*, 582.
- (6) Langer, L.; Bayot, V.; Grivei, E.; Issi, J.-P.; Heremans, J. P.; Olk, C. H.; Stockman, L.; Haesendonck, C. V.; Bruynserade, Y. *Phys. Rev. Lett.* **1996**, *76*, 479–482.
- (7) Dai, H.; Wong, E. W.; Lieber, C. M. *Science* **1996**, *272*, 523–526.
- (8) Ebbesen, T. W.; Lezec, H. J.; Hiura, H.; Bennett, J. W.; Ghaemi, H. F.; Thio, T. *Nature* **1996**, *382*, 54–56.
- (9) Thess, A.; Lee, R.; Nikolaev, P.; Dai, H.; Petit, P.; Robert, J.; Xu, C.; Lee, Y. H.; Kim, S. G.; Rinzler, A.; Colbert, D. T.; Scuseira, G. E.; Tománek, D.; Fischer, J. E.; Smalley, R. E. *Science* **1996**, *273*, 483–487.
- (10) Tans, S. J.; Devoert, M. H.; Dai, H.; Thess, A.; Smalley, R. E.; Geerligs, L. J.; Dekker, C. *Nature* **1997**, *386*, 474–477.
- (11) Saito, R.; Dresselhaus, G.; Dresselhaus, M. S. *Phys. Rev. B* **1996**, *53*, 2044–2050.
- (12) Chico, L.; Crespi, V. H.; Benedict, L. X.; Louie, S. G.; Cohen, M. L. *Phys. Rev. Lett.* **1996**, *76*, 971–974.
- (13) Chico, L.; Benedict, L. X.; Louie, S. G.; Cohen, M. L. *Phys. Rev. B* **1996**, *54*, 2600–2606.

(14) Guo, T.; Nikolaev, P.; Thess, A.; Colbert, D. T.; Smalley, R. E. *Chem. Phys. Lett.* **1995**, *243*, 49–54.

(15) Barber, D. J.; Loudon, R. *An introduction to the properties of condensed matter*; Cambridge University Press: Cambridge, 1989.

(16) Due to the interaction with the substrate and the resulting cross-sectional deformation of nanotubes, the actual nanotube diameter and consequently the actual flexural rigidity could be somewhat larger than their apparent height in AFM images suggests. Cross-sectional deformations, however, are more likely to occur for tubes with fewer shells, i.e., comparatively small flexural rigidity. This compensates the former effect to some degree and is discussed in more detail in ref 17.

(17) Hertel, T.; Walkup, R.; Avouris, Ph. To be published.

(18) Banhart, F.; Ajayan, P. M. *Nature* **1996**, *382*, 433–435.

(19) Bernasconi, M.; Parrinello, M.; Chiarotti, G. L.; Focher, P.; Tosatti, E. *Phys. Rev. Lett.* **1997**, *76*, 2081–2084.

(20) Chopra, N. G.; Benedict, L. X.; Crespi, V. H.; Cohen, M. L.; Louie, S. G.; Zettl, A. *Nature* **1995**, *377*, 135–138.

(21) Ruoff, R. S.; Lorents, D. C. *Carbon* **1995**, *33*, 925–930.

(22) Jung, T. A.; Schlitter, R. R.; Gimzewski, J. K.; Tang, H.; Joachim, C. *Science* **1996**, *271*, 181–184.

(23) Gmelins Handbuch der Anorganischen Chemie. *Kohlenstoff Teil B*; Verlag Chemie: Weinheim, 1968.

(24) Rochefort, A.; Salahub, D. R.; Hertel, T.; Avouris, Ph. To be published.